Magnetic field effect on periodic stripe domains in nematic liquid crystals

A. Sparavigna,[1] O. D. Lavrentovich,[2] and A. Strigazzi[1]
[1]*Dipartimento di Fisica, Politecnico di Torino, Corso Duca degli Abruzzi 24, I-10129, Torino, Italy*
[2]*Liquid Crystal Institute and Physics Department, Kent State University, Kent, Ohio 44242*
(Received 24 March 1994; revised manuscript received 6 September 1994)

Hybrid aligned nematic films placed onto an isotropic fluid substrate exhibit an unusual periodic stripe domain structure that appears only when the thickness of the film is smaller than a few tenths of a micrometer. We investigated the effect of a magnetic field on the threshold between the periodic stripe domains and the aperiodic deformed structure of the director. As experimentally observed, a magnetic field applied along the stripe domains favors a nonperiodic state with the director undistorted in the horizontal plane. The experimental findings are confirmed by a theory that takes into account not only the usual type of the elastic distortions, but also the so-called saddle-splay elasticity. A comparison of the experimental and theoretical data allows one to estimate that the saddle-splay elastic constant K_{24} is of the same order of magnitude as the bulk elastic constants; this result agrees with independent studies of confined liquid crystal systems.

PACS number(s): 61.30.Gd, 68.10.Cr

Many condensed matter materials show self-organization in the form of stripe patterns. These include superconductors [1], Langmuir monolayers [2,3], ferrofluids [4,5], ferroelectrics [6], magnetic films [7,8], as well as liquid crystals subjected to an external field [9,10] or antagonistic boundary conditions [11–13]. In many cases [1–8] the stripe pattern is formed by two different thermodynamic phases and the modulation period is set by a competition between long-range repulsive interactions (which may be of electrostatic or magnetostatic origin) and short-ranged attractive forces (nonzero surface tension of the domain walls). In liquid crystalline systems [9,10], the stripe phase is a manifestation of a smooth variation of the vector part of the order parameter. The periodicity is set by the competition between an external orienting field and elastic forces.

A different type and mechanism of the periodic self-organization was found in thin submicrometer nematic films placed between two isotropic media when no external field is applied [11–13]. The two media are set in antagonistic molecular orientation at the two surfaces of the film: homeotropic at one boundary and planar at the other. Therefore, the nematic director **n**, which describes the preferred molecular orientation, is distorted in the vertical plane. For sufficiently thick films **n** is restricted to lie in the vertical plane; the configuration is known as a hybrid aligned nematic cell (HAN). The decrease in the film thickness results in the increase of the vertical curvature and the HAN structure becomes unstable. Quite surprisingly, the experiment [11] has revealed that starting with some threshold thickness, the equilibrium state is reached through the distortions out of the vertical plane. These distortions create a periodic HAN (PHAN) pattern in the film plane. The presence of both vertical and horizontal deformations means that the PHAN structure must be strongly influenced by the elastic constant K_{24}, which describes the saddle-splay deformations [11–13].

Only very recently the elastic constant K_{24}, introduced many years ago for smectic and nematic phases [14,15], was estimated experimentally for nematic liquid crystals [16,17], surfactant monolayers [18], and three-dimensional lamellar smectic phases [19]. In contrast to the standard positive elastic constants of bend, splay, and twist deformations, the saddle-splay constant can be either positive or negative [19,20]. In this work we study the role played by an in-plane magnetic field on the stripe structure in hybrid aligned nematic film both theoretically and experimentally. Our experiments have been made using the liquid crystal pentylcyanobiphenyl (5CB) (BDH Chemical Ltd. K15), which exhibits a nematic phase at room temperature. A small drop of nematic liquid crystal has been deposited on the isotropic fluid surface (glycerine, 99+% purity). The glycerine substrate provides tangential orientation of 5CB. The upper boundary of the nematic film is free with the normal easy orientation (homeotropic wall).

The samples were prepared in Petri dishes (diameter of 80–100 mm) at room temperature and placed on the stage of a polarizing microscope. The microscope was located between the two poles of an electromagnet, which provided a horizontal magnetic field (up to ~5 kG). The thickness of the film was estimated using the data on the film area and the weight of the nematic drop deposited onto the substrate. The HAN configuration is unstable with respect to the appearance of the periodic domain, as presented in Fig. 1(a): the threshold thickness shown in this figure is about 0.4 μm and the PHAN configuration is present in the thinner part of the film. In Fig. 1, the thick region is on the left. As discussed in a previous paper [13], the nematic film is not flat: this allows one to visualize the main peculiarities of the field action on the stripes. First, when the field is applied along the x axis, the threshold is shifted toward the thinner part of the film [see Figs. 1(b)–1(d)]. The threshold d_a in Fig. 1(d) for the highest field $H=2850$ G, is about 0.30 μm. Second, the wave numbers are practically uninfluenced by the magnetic field, but the threshold wave number changes because the threshold thickness changes. In Fig. 2 the wave numbers for different sam-

1063-651X/95/51(1)/792(4)/$06.00

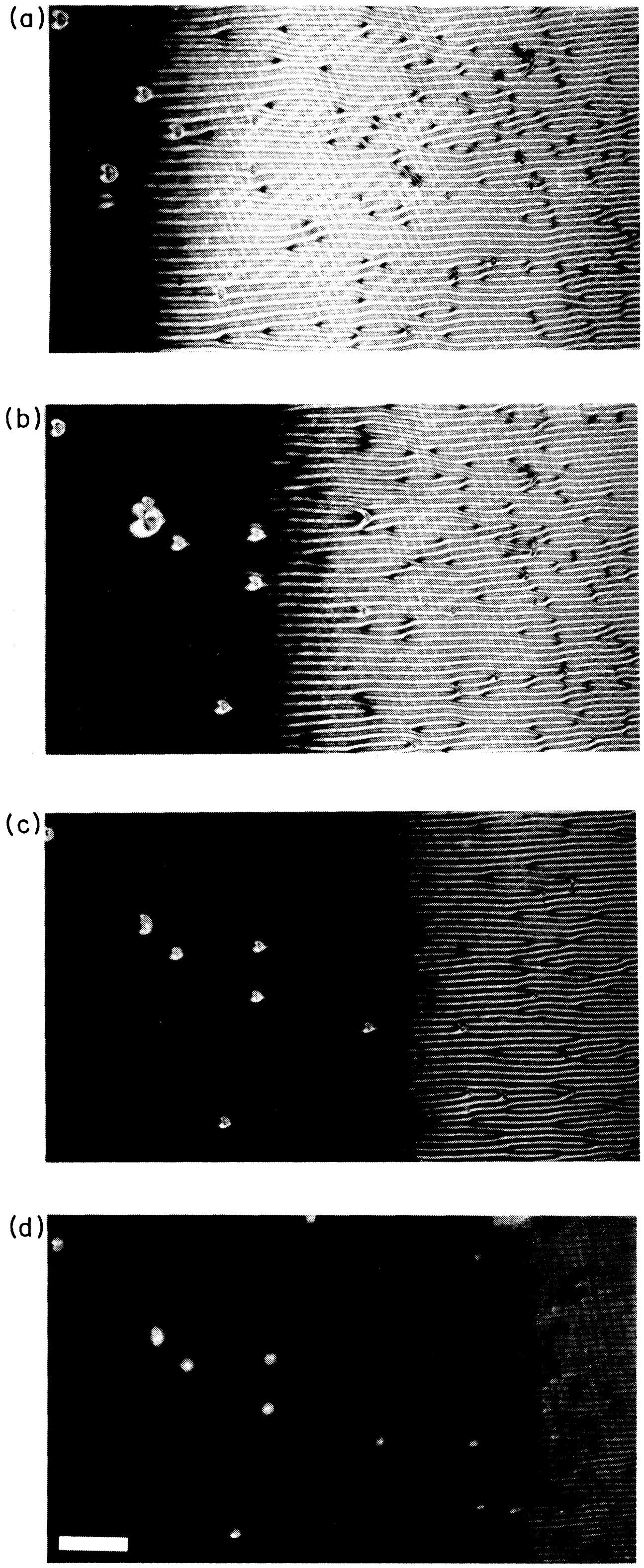

FIG. 1. Big 5CB drop viewed crossed polarizers. The PHAN-HAN line where the cell thickness is ~ 0.4 μm and the HAN structure is toward the drop center. (a) Zero field applied, (b) a field of 1620 G, (c) a field of 2438 G, and (d) a field of 2846 G. The bar corresponds to 150 μm.

ples and for different magnetic fields are shown as a function of the distance from the threshold position along the x axis. Let us compare these experimental results with a theoretical calculation of the threshold behavior and with the results previously obtained in Ref. [13].

We consider a nematic cell subjected to the in-plane magnetic field **H**. The elastic free energy density of Nehring and Saupe [15] and the magnetic field contribution are given, in the bulk isotropy approximation, by

$$f=\tfrac{1}{2}K\{(\mathrm{div}\mathbf{n})^2+(\nabla\times\mathbf{n})^2\} -(K+K_{24})\mathrm{div}[\mathbf{n}\,\mathrm{div}\mathbf{n}+\mathbf{n}\times\nabla\times\mathbf{n}]-\frac{\chi_a}{2}(\mathbf{n}\cdot\mathbf{H})^2\ , \quad (1)$$

where K is the common bulk elastic constant, K_{24} is the saddle-splay elastic constant, **n** is the nematic director, and χ_a is the magnetic susceptivity anisotropy. Let us assume a Cartesian reference frame $[xyz]$, $[xy]$ being the plane coincident with the homeotropic wall ($z_0=0$, where z is the coordinate normal to the substrates). The other wall, with planar orientation, is identified by $z_1=d$, d being the cell thickness. We assume that the initial orientation at this surface is parallel to the x axis and that a magnetic field is parallel to the $[x]$ direction, as in the experimental situation. The director **n** may be described by two angles in a polar reference frame $[\phi,\theta]$, where the azimuth ϕ is accounted for in the plane $[xy]$ from the x axis, while the polar angle θ is measured out of the plane $[xy]$. Hence

$$\mathbf{n}=\mathbf{i}\cos\phi\cos\theta+\mathbf{j}\sin\phi\cos\theta+\mathbf{k}\sin\theta\ . \quad (2)$$

If we are interested in studying the PHAN-HAN transition, we must work around the aperiodic deformed structure (HAN), applying a fluctuation on θ and ϕ around it. Since the value of θ in the HAN configuration is finite, we can linearize the bulk free energy and the surface contributions only on ϕ. The reduced bulk free energy density becomes

$$g_b=\frac{2f}{K}=\theta_y^2+\theta_z^2+(\phi_y^2+\phi_z^2)\cos^2\theta +2(\phi_y\theta_z-\theta_y\phi_z)\cos^2\theta -\frac{\chi_a}{K}H^2(1-\phi^2)\cos^2\theta\ , \quad (3)$$

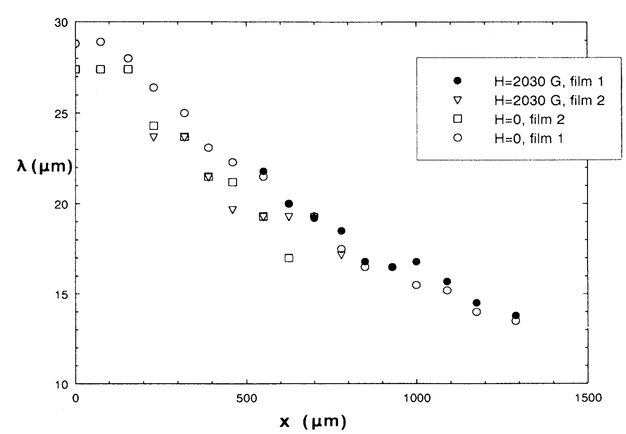

FIG. 2. PHAN pattern wavelength as a function of the x distance from the HAN-PHAN threshold in big droplets: experimental data on two different samples without field and with an applied field of 2030 G.

where the subscripts y,z refer to the derivatives with respect to the corresponding coordinates. The saddle-splay contribution to the reduced free energy density g_{ss} goes to the surface due to Gauss's theorem, giving rise to the term linearized on ϕ,

$$g_{ss}=2(1+\kappa_4)[-\phi_0\theta_{y0}+\tfrac{1}{2}\phi_{y0}\sin 2\theta_0 +\phi_1\theta_{y1}-\tfrac{1}{2}\phi_{y1}\sin 2\theta_1] , \quad (4)$$

where $\kappa_4\equiv K_{24}/K$ and the subscript $j=0,1$ refers to $z_0=0$ and $z_1=d$, respectively. Moreover, we have to add the contribution coming from the anchoring energy. In the Rapini-Papoular approach [21], the anchoring energy can be subdivided into a polar $[W_\theta]$ and an azimuthal $[W_\phi]$ part [13]: these contributions, after linearization on ϕ, can be written as

$$g_W=L_{\phi 0}^{-1}\phi_0^2\cos^2\theta_0-L_{\theta 0}^{-1}\sin^2\theta_0 +L_{\phi 1}^{-1}\phi_1^2\cos^2\theta_1+L_{\theta 1}^{-1}\sin^2\theta_1 , \quad (5)$$

where $L_{\phi j}^{-1}=W_{\phi j}/2K$ and $L_{\theta j}^{-1}=W_{\theta j}/2K$ are the de Gennes–Kléman extrapolation lengths.

The reduced free energy G is then obtained by means of the integral

$$G=\int_0^\lambda dy\int_0^d g_b(\theta_y,\phi_y,\theta_z,\phi_z)+\int_0^\lambda g_s(\theta_j,\phi_j,\theta_{yj},\theta_{yj})dy \quad (6)$$

with $g_s=g_{ss}+g_W$. λ is the wavelength of the periodic pattern, whose wave vector $\beta\equiv 2\pi/\lambda$ is parallel to the y axis, i.e., transverse to the tangential easy direction. We can obtain, from the free energy density the Euler-Lagrange equations,

$$\theta_{zz}+\theta_{yy}=h^{-2}\sin(2\theta) , \qquad \phi_{zz}+\phi_{yy}-2\theta_z\phi_z\tan\theta=h^{-2}\phi . \quad (7)$$

The boundary conditions are

$$\theta_{zj}+\tfrac{1}{2}L_{\theta j}^{-1}\sin 2\theta_j+\phi_{yj}R_j(\theta_j)=0 , \qquad -\phi_{zj}\cos^2\theta_j+L_{\phi j}^{-1}\phi_j\cos^2\theta_j+\theta_{yj}R_j(\theta_j)=0 , \quad (8)$$

where $h^2=(K/\chi_a)H^{-2}$ and $R_j(\theta_j)=\cos^2\theta_j-(1+\kappa_4)[1+\cos 2\theta_j]$ with $j=0,1$ at $z_0=0$ and $z_1=d$, respectively.

The problem to be solved is nonlinear, but can be easily treated numerically by subdividing the cell into n layers of equal thickness [13]. The insertion of this numerical solution into the boundary conditions (8) allows us to determine a dispersion relation giving the cell thickness d as a function $d(\beta,h,\kappa_4,L_{\theta j},L_{\phi j})$, where β is the wave vector and $h=(K/\chi_a)H^{-2}$ is the coherence length related to the reduced magnetic field.

The condition of a minimum of the reduced free energy allows us to to obtain the threshold thickness d_a between the period PHAN structure and the uniformly deformed structure HAN. In Fig. 3(a) the threshold d_a is reported as a function of the elastic ratio κ_4 for different values of the tilt anchoring strength $L_{\theta 1}$ on the planar boundary, with fixed $L_{\theta 0}$, when the azimuthal anchoring strengths $L_{\phi 0},L_{\phi 1}$ are negligible. In Fig. 3(b) the same threshold is shown for some values of $L_{\theta 1}$ without field and with an applied magnetic field H of 3 kG: the effect of H is a lowering of the threshold. In performing the calculation, we have assumed for the magnetic anisotropy the value of 1.2×10^{-7} (cgs) and for the elastic constant K a value of 0.7×10^{-6} dyn as measured for 5CB [22,23].

Due to the structure of the boundary conditions (8), the threshold thickness d_a is a function of κ_4, through the parameter $|R|=|1-2(1+\kappa_4)|=|1+2\kappa_4|$. The numerical analysis yields symmetrical results with respect to $R=0$ and the threshold d_a is a symmetric function with respect to $\kappa_4=-0.5$: for the sake of simplicity, we have shown the results in Fig. 3 only for $\kappa_4>-0.5$.

The symmetry with respect to $-|K+2K_{24}|$ and $+|K+2K_{24}|$ is not surprising and can be easily seen discussing the curvature [24] of the director field in the sample. Let us use a "smectic" analogy and rewrite the elastic free energy using the radii R_1 and R_2 of the curvature of the equidistant planes which are perpendicular to $\mathbf{n}$:

$$f=K\left[\frac{1}{R_1}+\frac{1}{R_2}\right]^2-2(K+K_{24})\frac{1}{R_1R_2} . \quad (9)$$

The term with K_{24} is related to the Gaussian curvature $G=1/(R_1R_2)$. R_1 and R_2 are algebraic quantities, so we can immediately see that we can reduce, by the same amount, the free energy with $+|K+2K_{24}|$ if $R_1R_2<0$ and with $-|K+2K_{24}|$ if $R_1R_2>0$.

As one can see from Fig. 3(b), the threshold between the HAN and the PHAN structure is lowered by the application of a magnetic field parallel to the $[x]$ direction. The important role played by the elastic ratio $\kappa_4=K_{24}/K$ is also evident, so that one can conclude that by knowing the anchoring strengths, the behavior of the PHAN-HAN threshold in a magnetic field can be useful for an estimation of the κ_4. In Ref. [13] we proposed an esti-

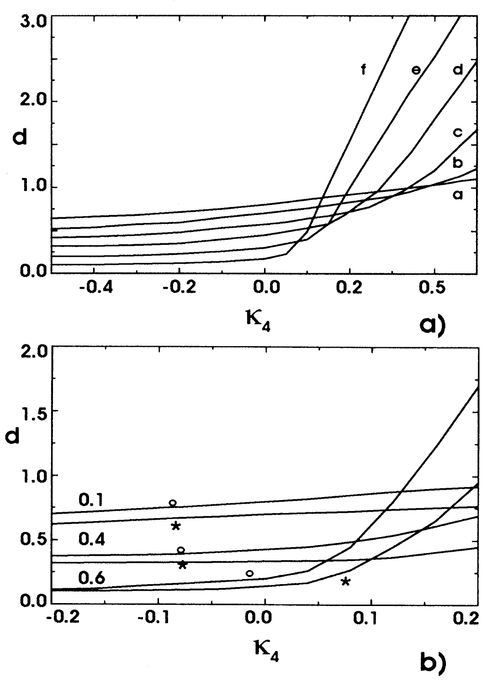

FIG. 3. Threshold thickness d_a between the PHAN and the HAN structure as a function of the elastic ratio $\kappa_4=K_{24}/K$. The value of $L_{\theta 0}$ is fixed to 0.7 μm, as previously estimated. (a) The behavior of d_a for different values of $L_{\theta 1}$ ranging from 0.1 (curve a) to 0.6 (curve f) with a step of 0.1 μm. (b) The behavior of d_a for $L_{\theta 1}=0.1$, 0.4, and 0.6 μm for $H=0$ (○) and 3 kG (∗). Note the lowering of the threshold due to the applied field.

mate of the ratio κ_4, substantially based on the study of the threshold d_p between the PHAN and the undistorted planar structure. Since it was difficult to estimate d_p, we assumed that it was different from zero, with an upper limit corresponding to $\sim 0.02\ \mu$m. By means of this assumption, the value of κ_4 was estimated to be $-0.012 < \kappa_4 < 0.0$ or $-1.00 < K_{24} < -0.988$, due to the symmetry with respect to $\kappa_4 = -0.5$.

Now we work only on the HAN-PHAN transition threshold and relax the assumption of the existence of the planar-PHAN threshold so that κ_4 can be *a priori* greater than 0. In fact, the theoretical analysis on the behavior of this threshold in a horizontal magnetic field suggests that the relevant influence of the magnetic field on the appearance of the periodic domains is more pronounced for κ_4 positive. For our theoretical calculations, whose results are presented in Fig. 3, we used a value for $L_{\theta 0}$ of $0.7\ \mu$m, as in the previous work.

Our experimental observations tell us that the total threshold thickness variation from a 0- to a 3-kG field is of about $0.1\ \mu$m and the threshold at zero field is about $0.4\ \mu$m: by simple inspection of Fig. 3(b) one can conclude that the best agreement between experimental observations and theoretical calculation happens in the case of $L_{\theta 1} = 0.4\ \mu$m for values of κ_4 between -0.05 and 0.05 or for $-1.05 < \kappa_4 < -0.95$.

One can conclude that the value of κ_4 is in agreement with the previous estimate, but the uncertainty is much higher now; this is due to the difficulty of estimating the real profile of the film. As discussed in Ref. 13, the nonflat profile of the film leads to additional azimuthal anchoring. As a result, films with different profiles can show different threshold thicknesses d_a. In our calculations we have assumed that the geometric anchoring is negligible so that the extrapolation length $L_{\phi j}$ is infinity: this is possible because the influence of these parameters in the determination of the threshold thickness is within the uncertainty of the experimental estimation of the threshold itself. That is, assuming $10\ \mu\text{m} < L_{\phi j} < \infty$, as is true for the geometrical anchoring [12], the threshold changes of about 5%: this is lower than the experimental error.

In conclusion, the present estimate κ_4 is in agreement with our previous one [13] and with the one given in Ref. [16]. In comparing our result with the one in Ref. [16], we make the following remark. The strip-domain effect should be insensitive to the sign of the whole saddle-splay term, as we have previously seen: this can be easily understood by considering the presence of positive and negative Gaussian curvature in the stripe domain. As a consequence, we obtain a symmetric threshold d_a with respect to $\pm|K+2K_{24}|$ (or in the notation of Ref. [16] $\pm|K+K'_{24}|$). So we obtain two estimates for the saddle-splay constant because we are dealing with the absolute value of $|K+2K_{24}|$ or $|K+K'_{24}|$. In the case of Ref [16], the authors evaluated K'_{24} by studying the director configuration in a cylindrically shaped sample, thus having only one sign of the Gaussian curvature and so a well defined sign of K'_{24}. The order of magnitude is comparable to the bulk elastic constant, as in our case.

One of us (O.D.L.) thanks the National Science Foundations for support [Grant No. DMR 89-20147 (ALCOM)] as well as the Laboratoire de Physique des Solides (CNRS) Orsay, France, where part of the work was performed.

[1] L. D. Landau, Zh. Eksp. Teor. Fiz. **13**, 377 (1943) [Sov. Phys. JETP **7**, 99 (1943)].
[2] H. Mohwald, Rep. Prog. Phys. **56**, 653 (1993).
[3] D. Andelman, F. Brochard, C. M. Knobler, and F. Rondelez, in *Micelles, Membranes, Microemulsions and Monolayers,* edited by W. M. Gelbart, A. Ben-Shaul, and D. Roux (Springer, Berlin, 1993).
[4] R. E. Rosensweig, *Ferrohydrodynamics* (Cambridge University Press, Cambridge, England, 1989), Chap. 7.6.
[5] A. J. Dickstein, S. Erramilli, R. E. Goldstein, D. P. Jackson, and S. A. Langer, Science **261**, 1012 (1993).
[6] T. Mitsui and J. Furuichi, Phys. Rev. **90**, 193 (1953).
[7] P. Molho, J. P. Porteseil, Y. Souche, J. Gouzerh, and J. C. S. Levy, J. Appl. Phys. **61**, 4188 (1987).
[8] M. Seul, L. R. Monar, L. O. Gorman, and R. Wolfe, Science **254**, 1616 (1991); M. Seul and R. Wolfe, Phys. Rev. Lett. **68**, 2460 (1992).
[9] R. B. Meyer, Phys. Rev. Lett. **22**, 918 (1969); Yu. P. Bobylev and S. A. Pikin, Zh. Eksp. Teor. Fiz. **72**, 369 (1977) [Sov. Phys. JETP **45**, 195 (1977)]; F. Lonberg and R. B. Meyer, Phys. Rev. Lett. **55**, 718 (1985).
[10] D. W. Allender, R. M. Hornreich, and D. L. Johnson, Phys. Rev. Lett. **59**, 2654 (1987); D. W. Allender, B. J. Frisken, and P. Palffy-Muhoray, Liq. Cryst. **5**, 735 (1989).
[11] O. D. Lavrentovich and V. Pergamenshchik, Mol. Cryst. Liq. Cryst. **179**, 125 (1990); V. M. Pergamenshchik, Phys. Rev. E **47**, 1881 (1993).
[12] A. Sparavigna, L. Komitov, O. D. Lavrentovich, and A. Strigazzi, J. Phys. II **2**, 1881 (1992), and references therein.
[13] A. Sparavigna, O. D. Lavrentovich, and A. Strigazzi, Phys. Rev. E **49**, 1344 (1994).
[14] W. Helfrich, Z. Naturforsch. C **28**, 693 (1973).
[15] J. Nehring and A. Saupe, J. Chem. Phys. **54**, 337 (1971); **56**, 5527 (1972).
[16] D. W. Allender, G. P. Crawford, and J. W. Doane, Phys. Rev. Lett. **67**, 1442 (1991); G. P. Crawford, D. W. Allender, and J. W. Doane, Phys. Rev. A **45**, 8693 (1992).
[17] R. J. Ondris-Crawford, G. P. Crawford, S. Zumer, and J. W. Doane, Phys. Rev. Lett. **70**, 194 (1993).
[18] B. Farago, D. Richter, J. S. Huang, S. A. Safran, and S. T. Milner, Phys. Rev. Lett. **65**, 3348 (1990).
[19] P. Boltenhagen, O. D. Lavrentovich, and M. Kléman, J. Phys. II (France) **1**, 1233 (1991); Phys. Rev. A **46**, 1743 (1992).
[20] H. Kellay, J. Meunier, and B. P. Binks, Phys. Rev. Lett. **70**, 1485 (1993).
[21] A. Rapini and M. Papoular, J. Phys. (Paris) Colloq. **30**, C1-54 (1969).
[22] B. J. Frisken, J. F. Carolan, P. Palffy-Muhoray, J. A. Pereboom, and G. S. Bates, Mol. Cryst. Liq. Cryst. Lett. **3**, 57 (1986).
[23] M. J. Bradshaw, E. P. Raynes, J. D. Bunning, and T. E. Faber, J. Phys. (Paris) **46**, 1513 (1985).
[24] M. Kléman, *Points, Lines, Parois* (Editions Physique, Paris, 1977).

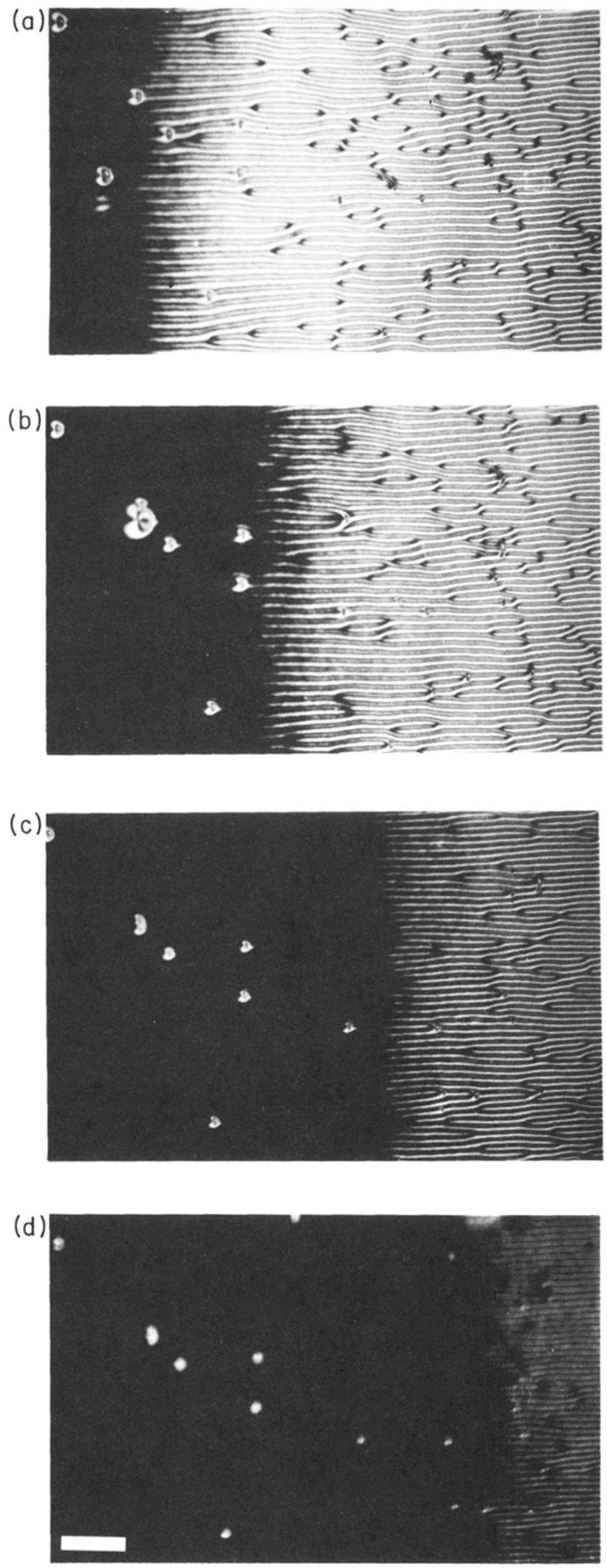

FIG. 1. Big 5CB drop viewed crossed polarizers. The PHAN-HAN line where the cell thickness is $\sim 0.4\ \mu$m and the HAN structure is toward the drop center. (a) Zero field applied, (b) a field of 1620 G, (c) a field of 2438 G, and (d) a field of 2846 G. The bar corresponds to 150 μm.